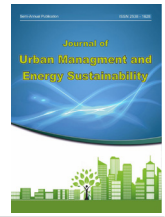
International Journal of Urban Management and Energy Sustainability (IJUMES)

Homepage: http://www.ijumes.com



ORIGINAL RESEARCH PAPER

Effects of Various Turbulence Models on The Accuracy and Efficiency of A Two-phase Method For Studying Pollutant Dispersion in Urban Street Canyons

Mehdi Ahmadi, Seyed Ali Agha Mirjalily*

Department of Mechanical Engineering, Ya.C., Islamic Azad University, Yazd, Iran

ARTICLE INFO

Article History:
Received 2026-04-11
Revised 2026-05-28
Accepted 2026-10-18

Keywords:
Computational fluid dynamics; Hybrid RANS/LES; large eddy simulation; pollutant dispersion; street canyon

ABSTRACT

Air pollution in dense urban areas threatens public health, and street canyons, where pollutants accumulate under weak ventilation, are a critical setting for exposure assessment. Computational fluid dynamics is widely used to predict pollutant dispersion there, but the turbulence model governs both the accuracy and the cost of the prediction, and comparisons of Reynolds-averaged Navier–Stokes, large eddy simulation and hybrid RANS/LES approaches within a two-phase framework remain scarce. This study aims to identify an appropriate turbulence model for simulating pollutant dispersion in a three-dimensional urban street canyon. The standard k–ε model, the Smagorinsky sub-grid-scale model and a hybrid model that applies k–ε near the walls and LES in the outer flow were implemented in an in-house finite-volume code. Air and carbon dioxide were treated as separate phases, the interface was captured with the volume-of-fluid method, and convective fluxes were discretised with the second-order Van Leer scheme under isothermal conditions at Re = 50,000. The models were validated against wind-tunnel data. LES and the hybrid model resolved two counter-rotating vortices in the upstream canyon and faster pollutant removal, whereas the k–ε model predicted a single vortex and pollutant accumulation near the walls and corners. The hybrid model required 5.14 times less computing time than LES but 4.35 times more than the k–ε model. The hybrid model therefore offers the best balance between accuracy and computational cost for two-phase pollutant dispersion in street canyons, while LES remains the reference when accuracy is paramount.

DOI: 10.22034/ijumes.2026.2108004.1417

Running Title: Studying Pollutant Dispersion In Urban Street Canyons

NUMBER OF REFERENCES	NUMBER OF FIGURES	NUMBER OF TABLES
64	08	04

*Corresponding Author:
Email: *Saa_mirjalily@iau.ac.ir*
Phone: 00989131530798
ORCID: https://orcid.org/0000-0002-1490-4380

INTRODUCTION

Nowadays, the air pollution issue has turned into one of the biggest problems, especially in big cities, which has certain drawbacks on human health, the environment, and the economy (Brook et al., 2004; World Health Organization, 2000). Turbulent wind flow around buildings in urban areas is one of the best cases to evaluate the accuracy and efficiency of turbulence models due to physical complexities such as sharp corners, ground effect, various vortices formations, and other factors (Abd Razak et al., 2013; Gao et al., 2009). The study of pollutant dispersion around buildings has become one of the most important research topics due to the increasing concerns about human health risks due to air pollution in recent decades (Nardell et al., 1991). To ensure that the concentration of pollutants does not exceed the permitted level for human health, designers must estimate how pollutants spread around the buildings in a street canyon (Deng et al., 2019; Riley et al., 1978; Xie et al., 2006).

Although many of these studies have relied on wind-tunnel and water-channel measurements (Blocken et al., 2008; Blocken et al., 2016; Karra et al., 2017; Khayrullina et al., 2017; Li et al., 2008; Neophytou et al., 2014; Partridge & Linden, 2013; Pournazeri et al., 2012; Ricci et al., 2017; Tsang et al., 2012), numerical simulations are less expensive and faster to perform (American Institute of Aeronautics and Astronautics, 1998). To study the dispersion of pollutants in street canyons the computational fluid dynamics (CFD) has been widely applied. CFD provides detailed information over the whole computational domain, and its main advantage is full control of the flow variables and boundary conditions at every node of the domain. For achieving accurate and reliable CFD results, a validation for the study is mandatory and the results must satisfy certain criteria (Allegrini & Carmeliet, 2018). There are many CFD approaches in the simulation of flow around buildings. A review of the literature shows that Large Eddy Simulation (LES) and Reynolds-Averaged Navier-Stokes simulations (RANS) are the two most popular methods in this field (An et al., 2013; Anderson, 1995; Antoniou et al., 2017). Most such studies have used RANS models to simulate pollutant distribution (Ahmadi et al., 2019; Awbi & Setrak, 1986; Blocken et al., 2007; Tian et al., 2006), while LES models are more suitable for estimating the wind flow in the atmospheric boundary layer and the dispersion of pollutants in the domain. Because LES resolves the time-dependent large-scale eddies, it captures the inherently unsteady flow around buildings, such as separation, recirculation and vortex shedding, more accurately than steady RANS models. For many years, LES, which can substantially improve flow prediction, was the main alternative to RANS (Abdalla et al., 2007; Baetke et al., 1990; Baker, 2007; Bazdidi-Tehrani et al., 2013; He et al., 2017; Holmes et al., 2000; M. Wang et al., 2012).

To overcome the weaknesses of LES and RANS, hybrid RANS/LES methods have become an increasingly popular strategy in turbulent-flow simulation (Meroney & Derickson, 2014; Meroney, 2016; Tominaga & Stathopoulos, 2016; Xu et al., 2017). Their basic idea is to retain the accuracy of LES while reducing the computational cost. The main aim of hybrid LES/RANS simulations is to apply RANS equations in the inner layer near walls to avoid the need for an excessively fine grid required by the LES, whereas the LES equations are solved in the outer layer of a boundary layer (Allmaras et al., 2012; Mockett et al., 2018; Shur et al., 2015). Detached-eddy simulation (DES), one of the first hybrid RANS/LES models, was proposed by Spalart et al. (1997). In recent years, many types of research have been carried out to study the dispersion of pollutants around buildings. Tominaga and Stathopoulos (2010) compared several k–ε models and the Smagorinsky LES model with experimental results. They concluded that the standard k–ε model does not have sufficient accuracy to estimate the pollutant concentration. However, models such as k–ε RNG and k–ε Realizable showed better compatibility with experimental results. They also stated that

the accuracy of the Smagorinsky averaged results are better than the results of the k–ε models. The spread of gaseous pollutants around a cube-shaped building was studied by Gousseau et al. (2011). They used the Smagorinsky model for simulation and compared their findings with the results obtained from the wind tunnel. They affirmed that the results of the wind tunnel and the Smagorinsky model are in excellent agreement. Evaluation of DES and DDES models in simulating turbulent wind flow on a building was performed by Jadidi and Heidarinejad (2013). The mentioned models were compared with turbulence models such as Smagorinsky and k–ε. The results showed that the DES model has higher accuracy than the RANS models and has a shorter iteration time than the LES model. They also stated that the DES model has good potential to simulate turbulent wind flows on the buildings. Huang et al. (2016) recently studied the effects of height and shape of the building rooftops on the pollutant dispersion and flow field inside an isolated street canyon. They used a two-dimensional numerical simulation for their research. Their results showed that the shape and the height of the building roofs have a strong impact on the vertical flow structure and pollutant distribution within an isolated canyon. In another study, air pollutant dispersion around high-rise buildings was simulated by Yu et al. (2017). They tested different roof shapes under different wind incidence angles. This research aimed to investigate the mechanisms behind the transition of the pollutant dispersion pathway. More recently, Ahmadi et al. (2020) treated the pollution as a separate phase and investigated a 3D incompressible turbulence model under isothermal conditions. They considered the hybrid RANS-LES method with a Sub-Grid Scale (SGS) technique within the framework of two-phase flow to study pollution distribution in urban street canyons.

The present paper continues this investigation by evaluating and comparing the application of the hybrid (RANS-LES) model against LES and RANS models on the mentioned case study. In RANS simulation, the standard two-equation k-ε turbulence model is employed, on the other hand, since no homogeneous direction exists in the flow in the hybrid (RANS-LES) method, the LES and Smagorinsky Sub Grid-Scale (SGS) model are implemented with standard k-ε turbulence model as RANS. Pollutant dispersion in an urban street canyon is simulated by these three models. In addition, although pollutant particles may be assumed in the same phase as air but for more details and better illustration, they are considered as a separated phase. Thus, in this study air is considered as the first phase and the pollutant (carbon dioxide) as the second phase. Unlike earlier comparisons, which treated the pollutant as a passive scalar, the three turbulence models are compared here within the same two-phase VOF framework and on the same three-dimensional street-canyon configuration, so that both their accuracy and their computational cost can be quantified. Also, to investigate the pollutant dispersion into the street canyon VOF method is utilized. The results can assist our understanding of the utilization of LES, hybrid (RANS-LES), and RANS method for simulation of pollutant distribution in urban street canyons. Moreover, the accuracy of each model can be evaluated, and the selected model can help future building design and pollutant distribution in urban street canyons. The results show that LES provides the most detailed information on the instantaneous fluctuations of the flow and the pollutant distribution in street canyons. It was also seen that the LES model spent the largest computing time, while the RANS model took the least. The computational time of the hybrid model was 5.14 times lower than that of LES but 4.35 times higher than that of the RANS model.

MATERIALS AND METHODS

In this paper, a practical comparison was done between hybrid RANS-LES, LES, and RANS turbulence models. For pollutant simulation, the two-phase method was utilized to the whole urban space as shown schematically in Figure 1. Build-

ing C2 is located upstream of C1, and C3 downstream of C1. The various sizes and dimensions of each building are presented in Table 1. This research aims to identify the differences between the above-mentioned models. The wind direction is considered to be orthogonal to the street canyon and the geometry is fixed along the street canyon direction. The computational dimensions are assumed as (4.0h×2.0h×1.0h), where h is the height of building C2 and is considered as the reference length scale with a value of h = 0.1 m. All buildings have a width of w=0.5h. Moreover, in the streamwise and spanwise directions, boundary conditions are set to be periodic for the whole domain, this configuration represents a demanding test case for model selection. Also, a constant pollutant concentration with an area source at the ground level of the first street canyon is considered (shown with red color in Figure 1). The inlet Reynolds number is defined with reference length (h) and reference velocity (U) as Re = Uh/ν, where ν is the kinematic viscosity. In this article, the inlet Reynolds number is fixed at Re = 50,000. (Tab. 1)

Table 1: Building dimensions in the computational domain.

Building	Height	Width	Length
C2	h	0.5h	0.5h
C1	0.5h	0.5h	2h
C3	2h	0.5h	0.5h

Finally, the volume of fluid (VOF) method is applied to capture the interface between the phases (Ahmadi & Khosravi Farsani, 2020; Aland & Voigt, 2012; Ding & Yuan, 2014; Hirt & Nichols, 1981; Soligo et al., 2019; Y. Wang et al., 2015; Y. Wang et al., 2018). The volume fraction of each phase is inserted as an additional variable in the governing equations. The well-known Finite Volume Method (FVM) is used to discretize the basic equations (Ferziger & Perić, 1996; Launder & Spalding, 1972; Patankar, 1980), and an in-house FORTRAN code was developed for the numerical solution of the case study based on the SIMPLEC algorithm. (Fig. 1)

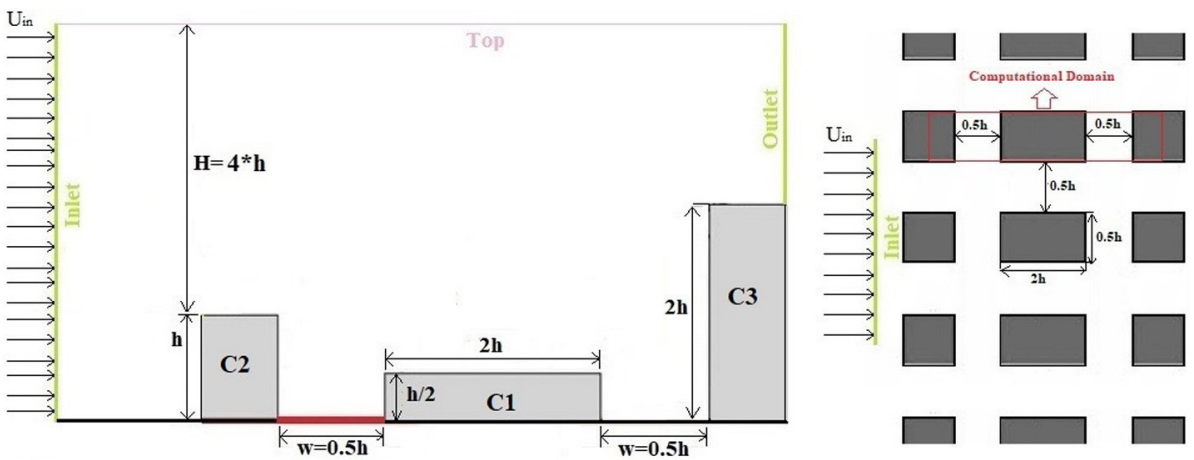


Figure 1: The geometry of problem.

Numerical method

Governing equations consist of a two-phase method for the numerical solution of the fluid flow and the dispersion equations. The main equations are derived from the Navier-Stokes equations, which are the basic principles of con-

tinuity and momentum conservations, and an extra equation is solved regarding the pollution concentration conservation. In addition, another equation is required for the description of the phase interfaces. All calculations are performed at a constant temperature of 300 K. Also, a 3D Cartesian co-ordinates system is applied in an unsteady, incompressible and isothermal flow of a Newtonian fluid.

Governing equations for the standard k_ε turbulence model are expressed as follows (Ferziger & Perić, 1996; Launder & Spalding, 1972; Patankar, 1980):

Continuity equation:

$$\frac{\partial \bar{U}_i}{\partial x_i}=0/ \quad (1)$$

momentum equation

$$\bar{U}_j\frac{\partial \bar{U}_i}{\partial x_j}=-\frac{1}{\rho}\frac{\partial \bar{P}}{\partial x_i}+\frac{\partial}{\partial x_j}(v\frac{\partial \bar{U}_i}{\partial x_j}-\overline{u_i u_j})+F_s \quad (2)$$

In equation (2) Fs is the volumetric representation of the surface tension force. Also U^-_j and U^-_i are the mean and fluctuating components of the velocity and Ui is the velocity in the xi-direction, Also in the above equations, P is the mean pressure, ρ is the density and υ is the kinematic viscosity of the fluid.

K and ε transport equations of the standard k_ε turbulence model are as follows:

$$\frac{\partial K}{\partial t}+\bar{U}_j\frac{\partial K}{\partial x_j}=\frac{\partial}{\partial x_j}\left(\frac{v_t}{\sigma_k}\frac{\partial K}{\partial x_j}\right)+v_t(\frac{\partial \bar{U}_i}{\partial x_j}+\frac{\partial \bar{U}_j}{\partial x_i})\frac{\partial \bar{U}_i}{\partial x_j}-\varepsilon \quad (3)$$

$$\frac{\partial \varepsilon}{\partial t}+\bar{U}_j\frac{\partial \varepsilon}{\partial x_j}=\frac{\partial}{\partial x_j}\left(\frac{v_t}{\sigma_\varepsilon}\frac{\partial \varepsilon}{\partial x_j}\right)+\frac{\varepsilon}{k}(C_{\varepsilon 1}v_t(\frac{\partial \bar{U}_i}{\partial x_j}+\frac{\partial \bar{U}_j}{\partial x_i})\frac{\partial \bar{U}_i}{\partial x_j}-C_{\varepsilon 2}\varepsilon) \quad (4)$$

Where:

$$\overline{u_i u_j}=\frac{2}{3}k\delta_{ij}-v_t(\frac{\partial \bar{U}_i}{\partial x_j}+\frac{\partial \bar{U}_j}{\partial x_i}) \quad (5)$$

$$v_t=C_\mu(\frac{k^2}{\varepsilon}) \quad (6)$$

K and ε are turbulent kinetic energy and turbulent dissipation rate. υ_t denotes the turbulent eddy viscosity, δ_{ij} is the Kronecker delta and C_μ=0.09, σk=1.0, σ_ε=1.314, $C_{\varepsilon 1}$=1.44, $C_{\varepsilon 2}$=1.92 are the default constants for the standard k–ε turbulence model. The above constants are obtained from fine and exact data fittings over a wide range of standard turbulent flows. The standard wall functions are applied for the near-wall flow. In the LES method, using a spatial filtering operation, the large scale and small-scale eddies of the flow will be separated, so the large-scale eddies are solved directly and the small-scale eddies are modeled and expressed as follows (Ferziger & Perić, 1996; Launder & Spalding, 1972; Patankar, 1980; You & Moin, 2007):

$$\frac{\partial \bar{U}_i}{\partial x_i}=0 \quad (7)$$

momentum equation:

$$\frac{\partial \bar{U}_i}{\partial t}+\bar{U}_j\frac{\partial \bar{U}_i}{\partial x_j}=-\frac{1}{\rho}\frac{\partial \bar{P}}{\partial x_i}+\frac{\partial}{\partial x_j}(v\frac{\partial \bar{U}_i}{\partial x_j}-\tau_{ij})+F_s \quad (8)$$

In equations (7 and 8), U^-_i is the filtered velocity and $P^-$is representing the pressure and not time-averaged values as in RANS equations. τ_{ij} is a tensor which represents due to the filtering operation, and it is assumed that small scales are more universal and isotropic than large scales. τ_{ij} is called the Sub Grid-Scale (SGS) stress and is calculated from:

$$\tau_{ij}-\frac{1}{3}\tau_{kk}\delta_{ij}=-2\mu_t\bar{S}_{ij} \quad (9)$$

$$\bar{S}_{ij}=\frac{1}{2}(\frac{\partial \bar{U}_i}{\partial x_j}+\frac{\partial \bar{U}_j}{\partial x_i}) \quad (10)$$

$$\mu_t=\rho L_s^2|\bar{S}| \quad (11)$$

$$|\bar{S}|=\sqrt{2\bar{S}_{ij}\bar{S}_{ij}} \quad (12)$$

$$L_s=min\,(kd,\ C_sV^{1/3}) \quad (13)$$

Where $\bar{S}_{ij}$ is the rate-of-strain tensor, μ_t the subgrid-scale turbulent viscosity, Ls the mixing length for the subgrid scales, k the Von Karman constant (k=0.4), d the closest wall distance, Cs the Smagorinsky constant, and V is the computational cell volume.

A linear interpolation based on the y+ value is used for switching between RANS (k_ε) and the LES model and it can be expressed as follows (Sajjadi et al., 2017):

(14)

$$\upsilon_t = \begin{cases} \upsilon_{t,LES} & if \quad y^+ > y^+_{up} \\ (1-\beta)\upsilon_{t,K-\varepsilon}+\beta\upsilon_{t,LES} & if \quad y^+_{down} < y^+ < y^+_{up} \\ \upsilon_{t,K-\varepsilon} & if \quad y^+ < y^+_{down} \end{cases}$$

$$\beta=\frac{y^+ - y^+_{down}}{y^+_{up} - y^+_{down}} \tag{15}$$

β is the weight factor and y_{down}^{+}, y_{up}^{+} are the lower and upper limits of the transition region which are selected as 60 and 300 (Patankar, 1980). Moreover, a convective-diffusive equation is assumed for calculation of pollutant concentration:

$$\frac{\partial C_i}{\partial t} + \frac{\partial (u_j C_i)}{\partial x_j} = \frac{\partial}{\partial x_j}\left(K\frac{\partial C_i}{\partial x_j}\right) + S_i \tag{16}$$

Where C_i is the pollutant concentration and K and Si are the diffusivity coefficient and the pollutant source, respectively. Also for all solid boundaries, the Von Neumann (zero-normal-gradient) conditions are considered. VOF method is an interface tracking technique for various phases, which has a conservative nature, and is expressed as follows (Hirt & Nichols, 1981):

$$\frac{\partial f}{\partial t} + \nabla.(\mathbf{u}f) - f\,\nabla.\mathbf{u} = 0 \tag{17}$$

In equation (17), u mentions the velocity vector, and *(f)* is the VOF function with a value between 0 and 1. Average values of density and viscosity at the interface are calculated and weighted with the function *f*:

$$\rho = f\rho_1 + (1-f)\rho_2 \tag{18}$$

$$\mu = f\mu_1 + (1-f)\mu_2 \tag{19}$$

Where ρ_1, ρ_2, μ_1, and μ_2 denote the density and viscosity of the phases. The equations (18 and 19) ensure mass conservation and play the role of the conservation law for the VOF function. In the momentum equations, F_s is the surface tension force and appears in the momentum equations as a volumetric force. It is modeled by the Continuum Surface Force (CSF) method (Brackbill et al., 1992). It also acts in the vicinity of the interfacial region and is expressed as (Ahmadi et al., 2020):

$$F_s = \gamma\kappa\nabla f \tag{20}$$

The interfacial tension γ is also assumed constant and the curvature of the interface (κ) is calculated from:

$$\kappa = \nabla.\frac{\nabla f}{|\nabla f|} \tag{21}$$

Solution procedure

Two-phase LES, Hybrid, and standard k-ε models were employed in this paper to simulate the turbulence effects. Discretization of the governing equations was carried out using the Finite Volume Method (Ferziger & Perić, 1996; Launder & Spalding, 1972; Patankar, 1980) on a fully structured grid to conduct the numerical solution procedure. For the momentum equation discretization in LES, a second-order upwind-central numerical scheme is utilized. For the standard k_ε model also, the second-order central differencing scheme was used to discretize the momentum equation, turbulent kinetic energy (k), and turbulent dissipation rate (ε) equations. Furthermore, for the time marching, the implicit second-order method is applied. In order to achieve more accurate results, the Second-order Van Leer approach was applied (Ahmadi & Khosravi Farsani, 2020; Ahmadi et al., 2020; van Leer, 1979). The SIMPLEC algorithm was also selected

to resolve the problem of velocity and pressure coupling. The TDMA and the Strongly Implicit Procedure (SIP) algorithms were utilized for pressure correction and the convergence criteria for all flow parameters were set at 10-6.

Grid Study

During the simulation process, grid refinement is one of the most important issues to acquire accurate and reliable results, especially near the walls and fluid phase boundaries. As was previously discussed a non-uniform and fully structured computational grid was selected. A maximum stretching ratio of 1.12 was applied to reduce the grid density in areas far away from the regions of interest. The Y+ value near the walls was reduced to less than 10 by making the grid finer due to the presence of larger gradients in the solution variables. To ensure the results are independent of the grid size, a coarse and a fine mesh were generated for each model and their details are presented in Table 2. (Tab. 2)

Table 2: Mesh details; h is the reference length, which is the building height of the inlet street canyon.

Grid	Number of elements (x × y × z)		Δxmin or Δzmin	Δymin
	Street canyon	Free surface layer		
coarse mesh (Hybrid)	140 × 60 × 80	140 × 60 × 70	4.19×10^{-3}h	8.56×10^{-3}h
fine mesh (Hybrid)	180 × 80× 120	180× 80 × 90	1.83×10^{-3}h	6.56×10^{-3}h
coarse mesh (LES)	180 × 80 × 120	180 × 80 × 90	1.83×10^{-3}h	9.85×10^{-3}h
fine mesh (LES)	260 × 120 × 160	260× 120 × 160	4.75×10^{-4}h	1.56×10^{-3}h
coarse mesh (k–ε)	90 × 40 × 60	90 × 40 × 40	9.11×10^{-3}h	9.85×10^{-3}h
fine mesh (k–ε)	120 × 60 × 90	120 × 60 × 70	6.12×10^{-3}h	8.56×10^{-3}h

The experimental wind tunnel results were selected for the grid study (Chavez et al., 2011). Figure 2 shows the comparison of normalized dilution on the rooftop of a building on the street canyon of Figure 1. As can be seen in Figure 2, the fine grid yields grid-independent results. (Fig. 2)

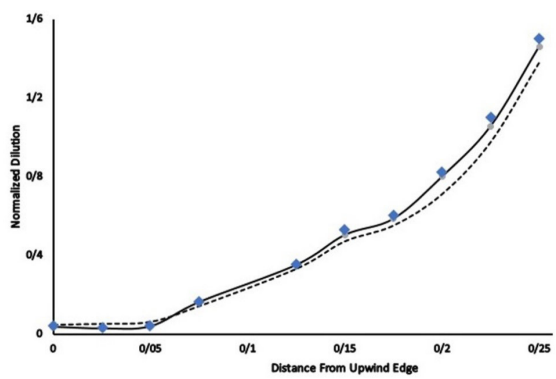


Figure 2: Comparison of normalized dilution on rooftop of a building on the street canyon as Figure 1. Calculation by current LES model and fine mesh; Calculation by the current k–ε model and fine mesh; ♦, Wind-tunnel experiment (Chavez et al., 2011).

Validation

After selecting the appropriate grid, the obtained numerical results were compared against experimental data from open literature (Rafailidis & Schatzmann, 1995). Dimensionless pollutant concentration, K, was compared on the leeward and windward walls with the available data. Figure 3 shows that the calculated results of all turbulence models are in good agreement with those obtained from the experiment although the predicted concentrations are slightly lower than the measured values. After this comparison, it can be concluded that the current turbulence models are capable of handling the flow and pollutant fields in the street canyons. Furthermore, Figure 2 can also be used as another validation for the results of this study against the obtained results by Chavez et al. (2011). (Fig. 3)

FINDINGS AND DISCUSSION

After selecting the appropriate grid and verifying the performance of the computer code, different

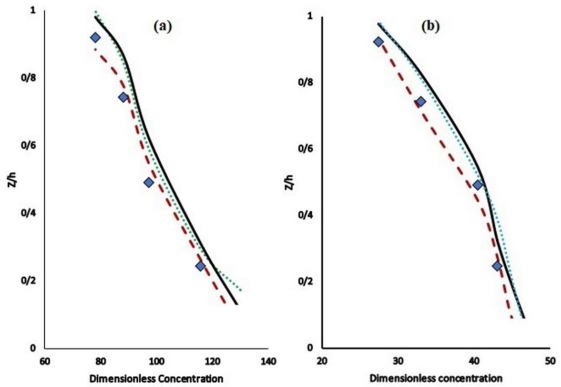


Figure 3: Distribution of dimensionless concentration, K, on the building walls of the street under different turbulence model. (a) Leeward side, (b) windward side. Calculation by the current LES; Calculation by the current hybrid model; Calculation by the current standard k–ε turbulence model; Wind-tunnel experiment (Rafailidis & Schatzmann, 1995).

runs were conducted with different models. The inlet Reynolds number (Re) is assumed to be constant at Re=50000 and the geometrical parameters are fixed for all cases. In the following sections, the comparisons of the results obtained by different turbulence models are presented. Also, the properties of phases are presented in Table 3. (Tab. 3)

The flow field comparison of LES, Hybrid, and k–ε models

Firstly, a general view of the computations in terms of streamline and velocity field is analyzed for the previously mentioned models. Based on the distribution of the streamlines and velocity contours, it was seen that there are different flow patterns in the street canyons. (Fig. 4)

Table 3: Properties of Air and Carbon dioxide at 30 oC.

	ρ(kg/m^3)	μ(kg/(m·s))
Air	1.17	$18.61*10^{-6}$
Carbon dioxide	1.98	$15.18*10^{-6}$

The flow field comparison of LES, Hybrid, and k–ε models

Firstly, a general view of the computations in terms of streamline and velocity field is analyzed for the previously mentioned models. Based on the distribution of the streamlines and velocity contours, it was seen that there are different flow patterns in the street canyons. (Fig. 4)

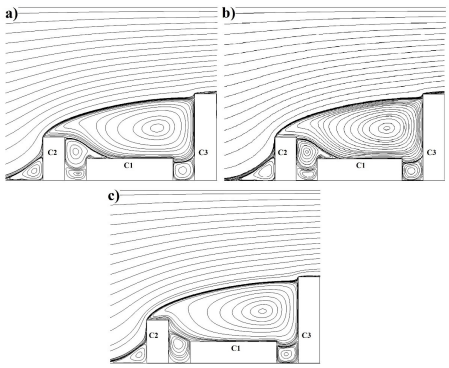


Figure 4: Streamlines a) LES, b) Hybrid and c) k–ε model at the centerline of geometry plan(y=0).

Figure 4 shows that a longitudinal vortex is formed at the top of the building C1 and is stretched on building C2. This longitudinal vortex is mainly driven by the shear stress of the free stream flow, and it leads to the generation of other vorticities in each street canyon. As shown in Figure 4, the streamlines in LES and Hybrid methods are quite similar and there is little difference between them but the k–ε model shows a major difference with them. The height of the longitudinal vortex which is predicted by the hybrid model is equal to that of predicted by LES and is larger than the k–ε model result. In the first street canyon, the hybrid and LES models predicted two counter-rotating vortices, and the first one is stretched at the top of building C1 but the k–ε model only predicted one vortex. (Fig. 5) In Figure 5 the predicted velocity magnitude is presented at the symmetry plan (y=0) for comparison. This comparative view of the results illustrates the significant difference in the velocity field behavior. In the flow domain, the best advantage of the LES model is its ability to cal-

culate the instantaneous velocity field which is not possible with the k–ε model. Also, the Hybrid model can predict the transient large-scale velocity fluctuations in the flow region, but the k–ε model fails to simulate them. It is seen that the hybrid model is capable of predicting the velocity field reasonably well, but not as well as the LES method, especially near the walls.

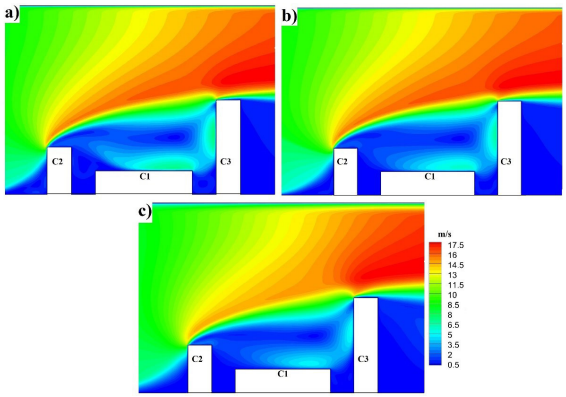


Figure 5: Velocity field a) LES, b) Hybrid and c) k–ε model at the centerline of geometry plan(y=0).

The second phase distribution and volume fraction comparison of LES, Hybrid, and k–ε models

Figure 6 shows that, for both the LES and hybrid models, the second phase spreads faster into the first street canyon and then discharges into the air whereas k–ε model predicts an accumulation of pollutants towards the corners, near the walls, and within the street canyon. This may be explained by the fact that LES and Hybrid models predict two counter-rotating vortices on the first street canyon and the upper clockwise vortex rotates much faster than the lower counter-clockwise vortex. Thus, it causes the rate of momentum transfer between the longitudinal vortex and the bottom vortex to be higher than the k–ε model. In contrast to LES, the k–ε model and, to a lesser extent, the hybrid model predicted low turbulence intensity at the bottom and near the wall regions. Besides, LES provides better results than the hybrid method because it captures transient mixing, as well as the dispersion and diffusion of the second phase as shown in Figure 6. From the study of streamlines and volume fractions as shown in Figures 4 and 6, it can be concluded that the second phase cannot spread into the second street canyon, and the pollutant exits from the first street canyon directly into the free streamflow. The main reason can be due to the geometrical parameters and

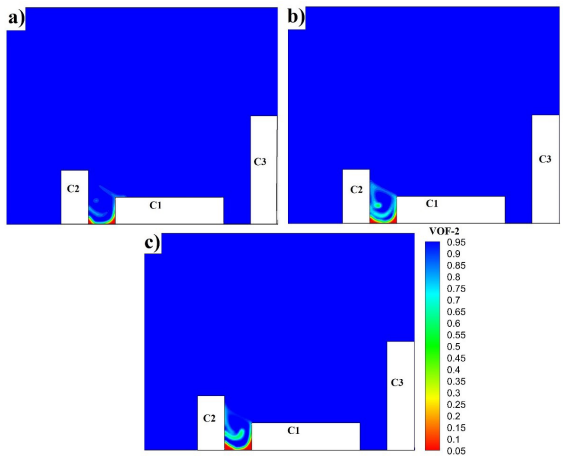


Figure 6: Distribution of phases a) LES, b) Hybrid and c) k–ε model at the centerline of geometry plan(y=0).

From Figure 7, the volume fraction of the second phase at leeward and windward sides of the first street canyon can be observed for different models. It can be noticed in Figure 7 that both k–ε and Hybrid models predicted an accumulation of pollutants more than LES towards the leeward and windward walls. This overprediction is more evident for the k–ε model. This can also be explained by the fact that the k–ε model and, to a lesser extent, the hybrid model underpredicted the circulation strength in the first street canyon and thus the lower maximum values of negative and positive velocities were predicted by this model as opposed to LES see (Fig. 6). (Fig. 7)

The grid size and time comparison of LES, Hybrid, and k–ε models

As noted previously, one of the main reasons for utilizing the hybrid model is to decrease the computational time in comparison with the LES model. The grid size used for different

models, as discussed in Section 2.3. For various models, the fine grid size was selected for reaching accurate results as shown in Table 2. It is seen that the required grid size for the k–ε model is less than the hybrid model which is on the other hand less than that for the LES model. The computational time for the volume fraction of the second phase in the first street canyon is shown in Table 4 and Figure 8 for different models. All calculations are done for different models on a dual-core computer. After the comparisons, it is seen that the LES consumes the longest time, while the k–ε model takes the least time amongst all. (Fig. 8)

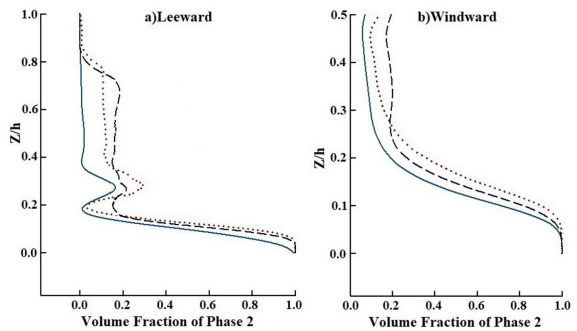


Figure 7: Leeward and Windward volume fraction of second phase at the centerline of geometry plan(y=0) on the building walls of the first street at different turbulence model. (a) Leeward side and (b) windward side. Calculation by the current LES; Calculation by the current hybrid model; Calculation by the current standard k–ε turbulence model.

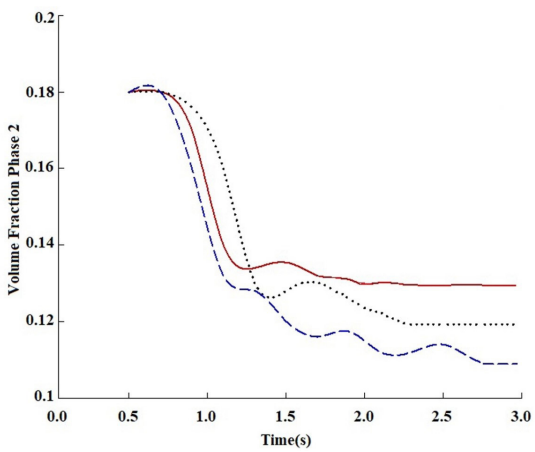


Figure 8: Volume fraction of phase 2 in the first street canyon. Calculation by the current LES; Calculation by the current hybrid model; Calculation by the current standard k–ε turbulence model.

In the two-phase flow field and pollutant simulation without losing any information on the results, the k–ε model required approximately 1.0 h (3,751 s), the hybrid model approximately 4.5 h (16,320 s) and LES approximately 23.3 h (83,871 s) on the same computer (Tab. 4). The computational time for the hybrid model was lower than the LES model by a factor of 5.14 but it was 4.35 times more than that of the k–ε model.

Table 4: Comparison of the computational times for different models.

Models	Computational time (s)
LES	83870.8
Hybrid	16320.1
k–ε	3751.2

RESULTS AND CONCLUSION

The aim of this research was to select an appropriate turbulence model for the pollutant dispersion in street canyons. For this reason three widely accepted turbulence models, namely, LES, Hybrid RANS /LES, and RANS models were applied to the case. In the RANS simulation, the two-equations standard k-ε turbulence model was employed, whereas in hybrid (RANS-LES), the LES and Smagorinsky Sub Grid-Scale (SGS) model along with the standard k-ε turbulence model as RANS were implemented. In the hybrid model, RANS equations were applied in the inner layer near walls to avoid the need for excessively fine grid whereas the LES equations are solved in the outer layer of a boundary layer. A two-phase simulation for the fluid flow and pollutant dispersion in an urban street canyon was simulated by these three models. To investigate the convective fluxes and the description of the interfaces the Volume of Fluid (VOF) method was utilized. Based on the presented result the following remarks were achieved:

•The Hybrid RANS/LES model predicted the flow field and pollutant distribution with good

accuracy at a reasonable computational cost and reproduced the two counter-rotating vortices in the upstream canyon predicted by LES.

•The computational time of the hybrid model for the two-phase pollutant simulation was 4.35 times that of the k–ε model but 5.14 times lower than that of LES.

•The predicted results of the hybrid method were less accurate than those of the LES method and more accurate than those of k-ε.

•The volume fraction of phases can be more accurately modeled by the LES model compared to the Hybrid model, but the computational cost of the LES model is several times higher than that of the Hybrid model.

In this regard, the Hybrid model provided information that cannot be obtained using the k-ε model. The findings can assist our understanding of the accuracy, computational time and cost of these three models. Moreover, the records of the present study can help to choose an appropriate model for future simulations of the effects of wind structure interactions on air pollutant dispersion around buildings. This study has limitations that point to future work. Carbon dioxide and air are miscible gases, so treating them as separate phases with the VOF method is a modelling simplification that should be compared with single-phase scalar-transport models. Only one canyon geometry, one wind direction and one Reynolds number were examined, and the validation was qualitative. Future studies should report quantitative validation metrics, such as the fraction of predictions within a factor of two of the observations (FAC2), the normalised mean square error (NMSE) and the fractional bias, and should consider other canyon aspect ratios, wind directions and thermal (non-isothermal) effects.

REFERENCES

Abd Razak, A., Hagishima, A., Ikegaya, N., & Tanimoto, J. (2013). Analysis of airflow over building arrays for assessment of urban wind environment. Building and Environment, 59, 56–65. https://doi.org/10.1016/j.buildenv.2012.08.007

Abdalla, I. E., Cook, M. J., Rees, S. J., & Yang, Z. (2007). Large-eddy simulation of buoyancy-driven natural ventilation in an enclosure with a point heat source. International Journal of Computational Fluid Dynamics, 21(5–6), 231–245. https://doi.org/10.1080/10618560701599710

Ahmadi, M., & Khosravi Farsani, A. (2020). Computational fluid simulation of non-Newtonian two-phase fluid flow through a channel with a cavity. Thermal Science, 24(2B), 1045–1054. https://doi.org/10.2298/TSCI180102151A

Ahmadi, M., Mirjalily, S. A. A., & Oloomi, S. A. A. (2019). A RANS k–ω simulation of 2D turbulent natural convection in an enclosure with heating sources. IIUM Engineering Journal, 20(1), 229–244. https://doi.org/10.31436/iiumej.v20i1.1040

Ahmadi, M., Mirjalily, S. A. A., & Oloomi, S. A. A. (2020). Simulation of pollutant dispersion in urban street canyons using hybrid RANS-LES method with two-phase model. Computers & Fluids, 210, Article 104676. https://www.sciencedirect.com/science/article/pii/S0045793020302474

Aland, S., & Voigt, A. (2012). Benchmark computations of diffuse interface models for two-dimensional bubble dynamics. International Journal for Numerical Methods in Fluids, 69(3), 747–761. https://doi.org/10.1002/fld.2611

Allegrini, J., & Carmeliet, J. (2018). Simulations of local heat islands in Zürich with coupled CFD and building energy models. Urban Climate, 24, 340–359. https://www.sciencedirect.com/science/article/pii/S221209551730010X

Allmaras, S. R., Johnson, F. T., & Spalart, P. R. (2012). Modifications and clarifications for the implementation of the Spalart–Allmaras turbulence model. In Proceedings of the Seventh International Conference on Computational Fluid Dynamics (ICCFD7) (Paper ICCFD7-1902). https://iccfd.org/iccfd7/assets/pdf/papers/ICCFD7-1902_paper.pdf

American Institute of Aeronautics and Astronautics. (1998). Guide for the verification and validation of computational fluid dynamics simulations (AIAA G-077-1998). AIAA.

An, K., Fung, J. C. H., & Yim, S. H. L. (2013). Sensitivity of inflow boundary conditions on downstream wind and turbulence profiles through building obstacles using a CFD approach. Journal of

Wind Engineering and Industrial Aerodynamics, 115, 137–149. https://doi.org/10.1016/j.jweia.2013.01.004

Anderson, J. D., Jr. (1995). Computational fluid dynamics: The basics with applications. McGraw-Hill.

Antoniou, N., Montazeri, H., Wigö, H., Neophytou, M. K.-A., Blocken, B., & Sandberg, M. (2017). CFD and wind-tunnel analysis of outdoor ventilation in a real compact heterogeneous urban area: Evaluation using "air delay". Building and Environment, 126, 355–372. https://doi.org/10.1016/j.buildenv.2017.10.013

Awbi, H. B., & Setrak, A. A. (1986). Numerical solution of ventilation air jet. In Proceedings of the 5th Symposium on the Use of Computers for Environmental Engineering Related to Buildings. CIBSE.

Baetke, F., Werner, H., & Wengle, H. (1990). Numerical simulation of turbulent flow over surface-mounted obstacles with sharp edges and corners. Journal of Wind Engineering and Industrial Aerodynamics, 35, 129–147.

Baker, C. J. (2007). Wind engineering—Past, present and future. Journal of Wind Engineering and Industrial Aerodynamics, 95, 843–870. https://doi.org/10.1016/j.jweia.2007.01.011

Bazdidi-Tehrani, F., Ghafouri, A., & Jadidi, M. (2013). Grid resolution assessment in large eddy simulation of dispersion around an isolated cubic building. Journal of Wind Engineering and Industrial Aerodynamics, 121, 1–15. https://www.sciencedirect.com/science/article/pii/S0167610513001347

Blocken, B., Stathopoulos, T., & Carmeliet, J. (2007). CFD simulation of the atmospheric boundary layer: Wall function problems. Atmospheric Environment, 41(2), 238–252. https://doi.org/10.1016/j.atmosenv.2006.08.019

Blocken, B., Stathopoulos, T., & Carmeliet, J. (2008). Wind environmental conditions in passages between two long narrow perpendicular buildings. Journal of Aerospace Engineering, 21(4), 280–287. https://doi.org/10.1061/(ASCE)0893-1321(2008)21:4(280)

Blocken, B., Stathopoulos, T., & van Beeck, J. P. A. J. (2016). Pedestrian-level wind conditions around buildings: Review of wind-tunnel and CFD techniques and their accuracy for wind comfort assessment. Building and Environment, 100, 50–81. https://doi.org/10.1016/j.buildenv.2016.02.004

Brackbill, J. U., Kothe, D. B., & Zemach, C. (1992). A continuum method for modeling surface tension. Journal of Computational Physics, 100(2), 335–354. https://doi.org/10.1016/0021-9991(92)90240-Y

Brook, R. D., Franklin, B., Cascio, W., Hong, Y., Howard, G., Lipsett, M., Luepker, R., Mittleman, M., Samet, J., Smith, S. C., & Tager, I. (2004). Air pollution and cardiovascular disease: A statement for healthcare professionals from the Expert Panel on Population and Prevention Science of the American Heart Association. Circulation, 109(21), 2655–2671. https://doi.org/10.1161/01.CIR.0000128587.30041.C8

Chavez, M., Hajra, B., Stathopoulos, T., & Bahloul, A. (2011). Near-field pollutant dispersion in the built environment by CFD and wind tunnel simulations. Journal of Wind Engineering and Industrial Aerodynamics, 99(4), 330–339. https://doi.org/10.1016/j.jweia.2011.01.003

Deng, Q., Deng, L., Miao, Y., Guo, X., & Li, Y. (2019). Particle deposition in the human lung: Health implications of particulate matter from different sources. Environmental Research, 169, 237–245. https://doi.org/10.1016/j.envres.2018.11.014

Ding, H., & Yuan, C.-J. (2014). On the diffuse interface method using a dual-resolution Cartesian grid. Journal of Computational Physics, 273, 243–254. https://doi.org/10.1016/j.jcp.2014.05.005

Ferziger, J. H., & Perić, M. (1996). Computational methods for fluid dynamics. Springer.

Gao, N. P., Niu, J. L., Perino, M., & Heiselberg, P. (2009). The airborne transmission of infection between flats in high-rise residential buildings: Particle simulation. Building and Environment, 44(2), 402–410. https://doi.org/10.1016/j.buildenv.2008.03.016

Gousseau, P., Blocken, B., & van Heijst, G. J. F. (2011). CFD simulation of pollutant dispersion around isolated buildings: On the role of convective and turbulent mass fluxes in the prediction accuracy. Journal of Hazardous Materials, 194, 422–434. https://doi.org/10.1016/j.jhazmat.2011.08.008

He, C., Liu, Y., & Yavuzkurt, S. (2017). A dynamic delayed detached-eddy simulation model for turbulent flows. Computers & Fluids, 146, 174–189. https://doi.org/10.1016/j.compfluid.2017.01.018

Hirt, C. W., & Nichols, B. D. (1981). Volume of fluid (VOF) method for the dynamics of free boundaries. Journal of Computational Physics, 39(1), 201–225. https://doi.org/10.1016/0021-9991(81)90145-5

Holmes, S. A., Jouvray, A., & Tucker, P. G. (2000). An assessment of a range of turbulence models when predicting room ventilation. In Proceedings of Healthy Buildings 2000 (Vol. 2, pp. 401–406).

Huang, Y.-D., Xu, X., Liu, Z.-Y., Deng, J.-T., & Kim, C.-N. (2016). Impacts of shape and height of building roof on airflow and pollutant dispersion inside an isolated street canyon. Environmental Forensics, 17(4), 361–379. https://doi.org/10.1080/15275922.2016.1230912

Jadidi, A. M., & Heidarinejad, G. (2013). Evaluating DES and DDES models for wind flow over building and comparing with traditional turbulence models. Modares Mechanical Engineering, 14, 81–93.

Karra, S., Malki-Epshtein, L., & Neophytou, M. K.-A. (2017). Air flow and pollution in a real, heterogeneous urban street canyon: A field and laboratory study. Atmospheric Environment, 165, 370–384. https://doi.org/10.1016/j.atmosenv.2017.06.035

Khayrullina, A., van Hooff, T., Blocken, B., & van Heijst, G. J. F. (2017). PIV measurements of isothermal plane turbulent impinging jets at moderate Reynolds numbers. Experiments in Fluids, 58(4), Article 31. https://doi.org/10.1007/s00348-017-2315-0

Launder, B. E., & Spalding, D. B. (1972). Lectures in mathematical models of turbulence. Academic Press.

Li, X.-X., Leung, D. Y. C., Liu, C.-H., & Lam, K. M. (2008). Physical modeling of flow field inside urban street canyons. Journal of Applied Meteorology and Climatology, 47(7), 2058–2067. https://doi.org/10.1175/2007JAMC1815.1

Meroney, R. N. (2016). Ten questions concerning hybrid computational/physical model simulation of wind flow in the built environment. Building and Environment, 96, 12–21. https://www.sciencedirect.com/science/article/pii/S0360132315301682

Meroney, R. N., & Derickson, R. (2014). Virtual reality in wind engineering: The windy world within the computer. Journal of Wind and Engineering, 11(2), 11–26.

Mockett, C., Haase, W., & Schwamborn, D. (Eds.). (2018). Go4Hybrid: Grey area mitigation for hybrid RANS-LES methods (Notes on Numerical Fluid Mechanics and Multidisciplinary Design, Vol. 134). Springer. https://doi.org/10.1007/978-3-319-52995-0

Nardell, E. A., Keegan, J., Cheney, S. A., & Etkind, S. C. (1991). Airborne infection: Theoretical limits of protection achievable by building ventilation. American Review of Respiratory Disease, 144, 302–306.

Neophytou, M. K.-A., Markides, C. N., & Fokaides, P. A. (2014). An experimental study of the flow through and over two-dimensional rectangular roughness elements: Deductions for urban boundary layer parameterizations and exchange processes. Physics of Fluids, 26(8), Article 086603. https://doi.org/10.1063/1.4892979

Partridge, J. L., & Linden, P. F. (2013). Validity of thermally-driven small-scale ventilated filling box models. Experiments in Fluids, 54, Article 1613. https://doi.org/10.1007/s00348-013-1613-4

Patankar, S. V. (1980). Numerical heat transfer and fluid flow. Hemisphere.

Pournazeri, S., Princevac, M., & Venkatram, A. (2012). Scaling of building affected plume rise and dispersion in water channels and wind tunnels—Revisit of an old problem. Journal of Wind Engineering and Industrial Aerodynamics, 103, 16–30. https://doi.org/10.1016/j.jweia.2012.01.006

Rafailidis, S., & Schatzmann, M. (1995). Study on different roof geometries in a simplified urban environment [Wind-tunnel data report]. Meteorological Institute, University of Hamburg.

Ricci, A., Burlando, M., Freda, A., & Repetto, M. P. (2017). Wind tunnel measurements of the urban boundary layer development over a historical district in Italy. Building and Environment, 111, 192–206. https://doi.org/10.1016/j.buildenv.2016.10.016

Riley, E. C., Murphy, G., & Riley, R. L. (1978). Airborne spread of measles in a suburban elementary school. American Journal of Epidemiology, 107(5), 421–432. https://doi.org/10.1093/oxfordjournals.aje.a112560

Sajjadi, H., Salmanzadeh, M., Ahmadi, G., & Jafari, S. (2017). Turbulent indoor airflow simulation using hybrid LES/RANS model utilizing lattice Boltzmann method. Computers & Fluids, 150, 66–73. https://www.sciencedirect.com/science/article/pii/S0045793017301093

Shur, M. L., Spalart, P. R., Strelets, M. K., & Travin, A. K. (2015). An enhanced version of DES with rapid transition from RANS to LES in separated flows. Flow, Turbulence and Combustion, 95(4), 709–737. https://doi.org/10.1007/s10494-015-9618-0

Soligo, G., Roccon, A., & Soldati, A. (2019). Mass-conservation-improved phase field methods for turbulent multiphase flow simulation. Acta Mechanica, 230, 683–696. https://doi.org/10.1007/s00707-018-2304-2

Spalart, P. R., Jou, W.-H., Strelets, M., & Allmaras, S. R. (1997). Comments on the feasibility of LES for wings, and on a hybrid RANS/LES approach. In Proceedings of the First AFOSR International Conference on DNS/LES. Greyden Press.

Tian, Z. F., Tu, J. Y., Yeoh, G. H., & Yuen, R. K. K. (2006). On the numerical study of contaminant particle concentration in indoor airflow. Building and Environment, 41(11), 1504–1514. https://doi.org/10.1016/j.buildenv.2005.06.006

Tominaga, Y., & Stathopoulos, T. (2010). Numerical simulation of dispersion around an isolated cubic building: Model evaluation of RANS and LES. Building and Environment, 45(10), 2231–2239. https://www.researchgate.net/publication/223403188_Numerical_simulation_of_dispersion_around_an_isolated_cubic_building_Model_evaluation_of_RANS_and_LES

Tominaga, Y., & Stathopoulos, T. (2016). Ten questions concerning modeling of near-field pollutant dispersion in the built environment. Building and Environment, 105, 390–402. https://www.sciencedirect.com/science/article/pii/S0360132316302347

Tsang, C. W., Kwok, K. C. S., & Hitchcock, P. A. (2012). Wind tunnel study of pedestrian level wind environment around tall buildings: Effects of building dimensions, separation and podium. Building and Environment, 49, 167–181. https://doi.org/10.1016/j.buildenv.2011.08.014

van Leer, B. (1979). Towards the ultimate conservative difference scheme. V. A second-order sequel to Godunov's method. Journal of Computational Physics, 32(1), 101–136. https://www.sciencedirect.com/science/article/abs/pii/0021999179901451

Wang, M., Lin, C.-H., & Chen, Q. (2012). Advanced turbulence models for predicting particle transport in enclosed environments. Building and Environment, 47, 40–49. https://www.sciencedirect.com/science/article/pii/S0360132311001661

Wang, Y., Shu, C., Shao, J. Y., Wu, J., & Niu, X. D. (2015). A mass-conserved diffuse interface method and its application for incompressible multiphase flows with large density ratio. Journal of Computational Physics, 290, 336–351. https://www.sciencedirect.com/science/article/pii/S0021999115001382

Wang, Y., Shu, C., Yang, L. M., & Yuan, H. Z. (2018). On the re-initialization of fluid interfaces in diffuse interface method. Computers & Fluids, 166, 209–217. https://www.sciencedirect.com/science/article/pii/S0045793018300768

World Health Organization. (2000). Air quality guidelines for Europe (2nd ed.). WHO Regional Office for Europe.

Xie, X., Huang, Z., & Wang, J. (2006). The impact of urban street layout on local atmospheric environment. Building and Environment, 41(10), 1352–1363. https://www.sciencedirect.com/science/article/pii/S0360132305002003

Xu, J., Li, M., & Gao, G. (2017). A dynamic hybrid RANS/LES approach based on the local flow structure. International Journal of Heat and Fluid Flow, 67, 250–260. https://www.sciencedirect.com/science/article/pii/S0142727X17308226

You, D., & Moin, P. (2007). A dynamic global-coefficient subgrid-scale eddy-viscosity model for large-eddy simulation in complex geometries. Physics of Fluids, 19(6), Article 065110. https://doi.org/10.1063/1.2739419

Yu, Y., Kwok, K. C. S., Liu, X. P., & Zhang, Y. (2017). Air pollutant dispersion around high-rise buildings under different angles of wind in-

cidence. Journal of Wind Engineering and Industrial Aerodynamics, 167, 51–61. https://doi.org/10.1016/j.jweia.2017.04.006

COPYRIGHTS

©2023 The author(s). This is an open access article distributed under the terms of the Creative Commons Attribution (CC BY 4.0), which permits unrestricted use, distribution, and reproduction in any medium, as long as the original authors and source are cited. No permission is required from the authors or the publishers.

HOW TO CITE THIS ARTICLE

Ahmadi, M. & Agha Mirjalily, S. A. (2026). Effects of Various Turbulence Models on The Accuracy and Efficiency of A Two-phase Method For Studying Pollutant Dispersion in Urban Street Canyons. (e743260). International Journal of Urban Management and Energy Sustainability, 7(2), e743260

DOI:10.22034/ijumes.2026.2108004.1417